Journal of Materials Chemistry C

ROYAL SOCIETY OF CHEMISTRY

REVIEW

View Article Online
View Journal | View Issue

Check for updates

Cite this: J. Mater. Chem. C, 2024, 12, 12692

Research progress in fluorescent gas sensors based on MOFs

Ruixiao Dong,†[ab] Zhengqi Shen,†[ab] Huizi Li,*[ab] Jiangong Cheng*[ab] and Yanyan Fu *[ab]

Received 14th June 2024,
Accepted 22nd July 2024

DOI: 10.1039/d4tc02491e

rsc.li/materials-c

Currently, the importance of gas sensing is rapidly gaining recognition in a multitude of domains, including environmental conservation, security measures, food safety protocols, and medical diagnostic processes. As the requirements for these applications continue to escalate, there is a corresponding upsurge in the demand for gas sensors that can provide improved sensing performance. Metal–organic frameworks (MOFs) are among the most promising materials for sensing applications, owing to their highly tunable porous structures and exceptionally high specific surface areas. In parallel, fluorescence sensing stands out as an exceptional technique due to its ultra-high sensitivity and rapid response time. Hence, the integration of MOF-based structures with fluorescent sensing, merging a state-of-the-art sensing material with an advanced technique, has exhibited remarkable performance in detecting a spectrum of gases, encompassing both inorganic and organic species. This review commences with a detailed exposition of the operational mechanisms underlying gas sensing based on the fluorescent MOF material. It proceeds to showcase the targeted applications of this technology within the realm of gas sensing, encompassing the detection of oxygen, nitrogen oxides (NO_x), sulfur oxides (SO_x), and an assortment of volatile organic compounds (VOCs). The review concludes with an in-depth discussion of the future prospects and the challenges faced in the advancement of MOF-based fluorescent gas sensing technologies.

Published on 26 Qado Dirri 2024. Downloaded by Fail Open on 23/07/2025 10:24:49 AM.

1. Introduction

Since the inception of the first gas sensor in the 1960s,[1] the need for substance identification through gaseous analysis has been on the rise. Gas sensors are now extensively applied in a multitude of domains, including environmental conservation,[2–4] industrial safety,[5,6] public security,[7–9] food safety,[10] and medical diagnostics.[2] With the emergence of new demands, the performance standards for gas sensors, notably in terms of sensitivity, selectivity, and stability, have become more stringent. This has driven researchers to pursue innovation in the creation of more superior sensing materials.

Metal–organic frameworks (MOFs) are porous structures that self-assemble from metal ions and organic ligands, with the smallest cyclic units formed by them, stacked and extended in space to form a three-dimensional ordered structure. The cyclic units are the so-called secondary building units (SBUs).[11] MOFs have garnered significant attention due to their unique characteristics.[12] The size-tunability of their porosity and their large specific surface area are particularly notable, making MOFs a highly promising material for applications in catalysis,[13,14] gas adsorption and separation,[15–18] biomedical research,[19] and sensing.[20–24] Applications of MOFs in the field of gas sensing have been extensively explored, with their advantages primarily stemming from the following aspects. Firstly, the extensive network of binding sites within the 3D pores of MOFs effectively facilitates interactions between the sensitive material and analyte molecules, thereby enhancing the sensitivity of the gas sensor.[25] Secondly, MOFs are characterized by their compositional flexibility, which allows for the enhancement of sensing capabilities by adjusting the building blocks or by incorporating functional groups into the framework, and offers a thin-film fluorescence gas sensor with high 3S (sensitivity, selectivity, and stability).[26–28] Lastly, the high degree of crystallinity inherent in MOF structures is a significant advantage, and comparison of the orderliness of the pore structure facilitates the selection of analyte molecules. This characteristic enables precise and accurate characterization of the MOFs' structural features, which is essential for understanding and optimizing the sensing mechanism at the molecular or atomic level.[29] Tailoring to the distinct transduction mechanisms characteristic of various MOF materials, an array of advanced gas sensing modalities has been conceived. This includes the development of chemoresistive sensors, ferroelectric sensors, mass-sensitive sensors, magnetic sensors and

[a] State Key Lab of Transducer Technology, Shanghai Institute of Microsystem and Information Technology, Chinese Academy of Sciences, Changning Road 865, Shanghai, 200050, China. E-mail: huizi.li@mail.sim.ac.cn, jgcheng@mail.sim.ac.cn, fuyy@mail.sim.ac.cnb

[b] Center of Materials Science and Optoelectronics Engineering, University of the Chinese Academy of Sciences, Yuquan Road 19, Beijing, 100039, China

† These authors contributed equally to this work.

This journal is © The Royal Society of Chemistry 2024

Published on 26 Qado Dirri 2024. Downloaded by Fail Open on 23/07/2025 10:24:49 AM.

fluorescent sensors.[30] Among the diverse range of MOF materials, fluorescent MOFs emerge as a particularly promising option for real-time trace gas detection, leveraging their rapid sensing response and high sensitivity. MOF materials also have a wide range of applications in the field of electrical sensing, but there is the problem of slow sensing and recovery rate; its response time and recovery time often need a few minutes to several tens of minutes, which is not suitable for sensing and detection of trace amounts of hazardous chemicals. For classical fluorescent probes such as organic fluorescent molecules and quantum dots, MOF materials show excellent advantages in gas adsorption due to their porous properties. At the same time, organic combination with many functional groups and ligands can also be realized.[31] Especially for the widely used organic fluorescent gas sensors, many organic fluorescent probes have an ACQ effect due to the large conjugated fluorophores, which will limit gas sensing in the solid phase. The MOF structure can also bring different prospects for such organic fluorescent probes. To date, a multitude of research articles have been published, showcasing the sensing applications of various fluorescent MOFs across different domains.[32–35] However, it is rarely that a comprehensive review is found that thoroughly examines the working mechanisms and practical applications of the latest fluorescent MOFs developed for gas sensing. In this review, we begin with a concise overview of the gas sensing mechanisms of fluorescent MOFs. Subsequently, we delve into the recent advancements in the application of fluorescent MOFs for sensing inorganic gases and volatile organic compounds (VOCs). Finally, we address the challenges and future prospects of fluorescent MOFs in the realm of gas sensing.

2. Mechanism of fluorescent MOFs for gas sensing

The working principle of fluorescent MOFs in gas sensing is fundamentally based on the fluorescence variation arising from the interaction between analyte gas and the luminescence system of MOFs. The luminescence mechanisms of fluorescent MOF materials are typically classified into two principal categories, as depicted in Fig. 1: intrinsic self-illumination from the MOF structure and embedding or modifying fluorescent moieties in the MOF matrix.

In self-illuminated MOF structures, the fluorescence signals typically arise from three distinct mechanisms: ligand-centered emission, metal-centered emission, and charge transfer interactions between the ligand and the metal ions.[36] Among them, ligand-centered emission stands out as the most prevalent luminescence mode and is typically observed in frameworks featuring aromatic or row-conjugated ligands.[37,38] In the context of sensing applications, the interaction of incoming analyte molecules with the MOFs can result in the disruption or distortion of the organic linkers within the MOF architecture. As a consequence, this perturbation leads to corresponding shifts in the fluorescence signal's emission intensity or spectral peak.[39,40] Secondly, in the realm of metal-centered emission, lanthanides and transition metals with d^{10} electron configurations are frequently employed as luminescent centers. For instance, when lanthanide ions are integrated as SBUs or introduced into the pores of MOFs, they can be sensitized by organic chromophores through an antenna effect, resulting in a characteristic fluorescence that is centered on the metal ions.[41]

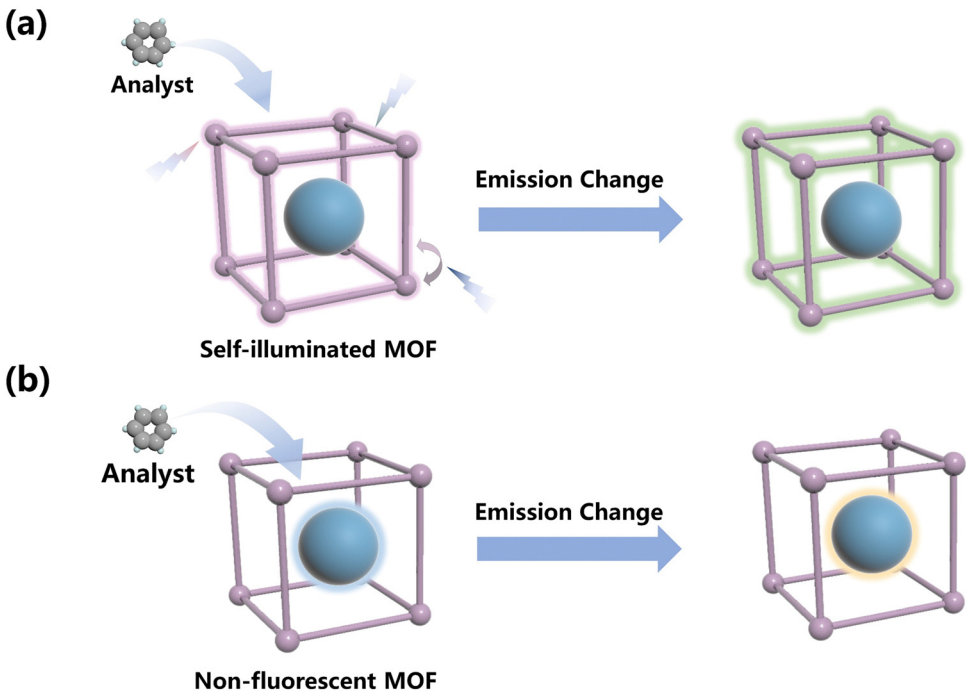

Fig. 1 The mechanisms of MOF sensing gas analysts.

Published on 26 Qado Dirri 2024. Downloaded by Fail Open on 23/07/2025 10:24:49 AM.

The final mechanism to consider is charge-transfer-based self-illumination. In the MOFs containing transition metal ions, charge transfer between the ligands and the metal ions is a common phenomenon. Depending on the presence or absence of d electrons in the valence orbitals, these charge transfer processes can be differentiated into two types: ligand-to-metal charge transfer (LMCT) and metal-to-ligand charge transfer (MLCT).[36]

Regarding MOFs that are inherently non-fluorescent, post-synthetic modification, achieved by incorporating or chemically modifying fluorescent moieties within the MOF lattice, represents an efficacious strategy.[42] By capitalizing on the MOFs' inherent porosity, these modifications can significantly bolster their fluorescence and sensing characteristics, rendering the MOF platform an effective tool for gas sensing applications. Some sensitive fluorescent materials are known for their commendable sensitivity or selectivity; however, their fluorescence intensity is markedly diminished in the aggregated state due to phenomena such as aggregated fluorescence quenching (ACQ). Upon integration into the MOF matrix, not only is the fluorescence intensity of these materials augmented, but their sensing capabilities for specific gases are also concurrently enhanced. This enhancement is attributed to the dispersive and protective attributes of the MOFs' cage-like structure, which mitigates the ACQ effect.[43] For instance, perylenes and their derivatives, which are particularly prone to ACQ and thus limited in sensing applications, can be strategically incorporated as organic linkers within the MOFs. By partially substituting non-fluorescent linkers of comparable length, a hybrid connector MOF is formed, allowing for effective modulation of perylene spacing to suppress ACQ and enhance the material's sensing performance for gases like oxygen.[44] Conversely, for fluorescent materials that exhibit favorable fluorescence characteristics in the solid state but lack sensitivity to analyte gases, the MOF framework, with its extensive specific surface area and multitude of active sites, offers an increased number of contact points with the sensitive materials. This feature can significantly amplify the sensor's sensing performance by facilitating more interactions between the sensing material and the target analytes.[45,46]

The conventional chemical sensing mechanisms of fluorescence-based gas sensing primarily encompass mechanisms such as fluorescence ''turn-off'' and ''turn-on'' induced by photoinduced electron transfer (PET), charge transfer (CT) and excited-state intramolecular proton transfer (ESIPT), *etc.*[47–52] Emerging fluorescent MOF based gas sensors adhere to these same foundational principles. Building upon these, and by capitalizing on the unique structural attributes of MOFs, fluorescent MOFs have achieved remarkable applications in the realm of gas sensing.

3. Applications of fluorescent MOF sensors in inorganic gases

3.1. Water vapor detection

It is well-established that the weak coordination bonds between metal ions and organic ligands in MOF structures render them highly susceptible to hydrolysis in aqueous environments.[53] This inherent poor water stability significantly restricts their application in high humidity conditions, including water sensing and water separation. However, recent advancements have demonstrated that the water stability of MOFs can be markedly enhanced by incorporating hydrophobic groups or applying hydrophobic coatings to the crystal surface.[18,54] Leveraging the unique aggregation and adsorption properties of MOFs enables effective sensing of water molecules in air. Materials based on MOF structures have been reported for the detection of trace water in solvents and air humidity.[55,56] Precise air humidity monitoring is essential in numerous fields, including agricultural production, the chemical industry, and everyday life.[57] To address the heightened demands for air humidity detection, fluorescent MOFs have been progressively optimized in terms of response time, detection range, and stability.

In the initial studies employing fluorescent MOFs for humidity sensing, the response time was commonly in the range of minutes, attributed to the gradual fluorescence alteration following the absorption of a critical mass of water molecules within the MOF pores. To transcend this limitation, researchers have demonstrated that the response time can be significantly reduced by engineering the MOF ligands to incorporate the ESIPT effect. Chen *et al.*[58] have developed a MOF featuring Zn as the metal center, complexed with the meticulously designed ligand H2hpi2cf. The ESIPT process brings forward unique dual emission in organic molecules by the fast switching between enol (E) and keto (K) tautomers, which is subject to subtle surrounding environmental disturbance on the intramolecular proton transfer and leads to tunable emission for PL sensing. The H-bonding between water and –OH group in hydrated LIFM-CL1-H_2O effectively hampers the excited state proton transfer to the imidazole N-atom. So LIFM-CL1-H2O displays blue emission at 463 nm in the solid state with higher quantum yield. In contrast, the dehydrated LIFM-CL1 does not interfere with intramolecular proton transfer, and is thus characteristic of keto emission (K*) owing to a normal ESIPT process (E–E*–K*–K–E), showing cyan emission at 493 nm with lower quantum yield (Φ_{PL} = 15%). This construct enables the ultrasensitive detection of water molecules, achieving a response time of within 2 seconds. This swift response is contingent upon the water-driven single-crystal-to-single-crystal (SC–SC) transition, an intricate physical process that, in tandem with the double optical switching emission mechanism underpinned by the ESIPT, permits each water molecule to distinctly alter the MOF crystal structure and its fluorescence emission profile. This advancement significantly enhances the speed of humidity detection, reducing the response time from a multi-minute duration to a matter of seconds, and provides a linear, fluorescence-based response to relative humidity levels spanning the 0–21% range.

Beyond the need for rapid response times, an extended detection range is equally sought-after for humidity sensors. Researchers have outlined three key approaches to broaden this range: the optimization of water-sensitive fluorescent moieties, the employment of the fluorescence based ratiometric sensor, and the fine-tuning of the MOF's macrostructure.

 This journal is © The Royal Society of Chemistry 2024

Published on 26 Qado Dirri 2024. Downloaded by Fail Open on 23/07/2025 10:24:49 AM.

Carbon dots (CDs) have emerged as a promising fluorescent moiety, notable for their adjustable emission wavelengths through the alteration of the excitation light's wavelength.[59,60] In a recent study, Wu[61] and colleagues introduced red-emitting CDs into an indium-based metal–organic framework (In-MOF) and subsequently modified the MOF with green-emitting terbium (Tb^{3+}) ions post-synthesis, yielding a hybrid material with dual-emission characteristics. The MOF's skeletal structure provides a separation effect that efficiently curbs the agglomeration of carbon dots. When Tb^{3+}@p-CDs/MOF composites are irradiated with a laser beam at 360 nm, the material dispersed in the ethanol solution produces both red and green light, but the luminous intensity of the p-CDs is stronger and eventually shows a red luminescent color, while dispersed in the aqueous solution, due to agglomeration effects, which leads to red light quenching, finally leaving only green light and thus showing the green colour. The concurrent presence of these two fluorescent species expands the material's humidity detection range, successfully achieving a detection span from 33% to 85.1% relative humidity.

The ratiometric fluorescent sensor, which exhibits heightened sensitivity to humidity fluctuations compared to the fluorescence intensity variation at a single wavelength, represents an alternative and effective methodology for extending the humidity detection spectrum. Researchers have designed and demonstrated the ratio meter sensor based on upconversion emission fluorescent MOFs with lanthanide metals as the centers. Wang[62] and colleagues have integrated lanthanide rare earth elements into the MOF framework, successfully creating an upconversion luminescent Y/Yb/Er-MOF for an extended range of water vapor detection. This innovative material utilizes two luminescent centers: Yb^{3+} and Er^{3+}. During the upconversion luminescence process of the MOF, the emission wavelength of Yb^{3+} ions matches the absorption wavelength of Er^{3+} ions. As a result, upon excitation, Yb^{3+} ions can efficiently transfer energy to Er^{3+} ions, inducing fluorescence emission from the Er^{3+}. In the vicinity of water molecules, the high-energy –OH vibrational mode of water can intercept a portion of the energy destined for the Er^{3+} ions from the excited state of Yb^{3+}. This interception results in the quenching of upconversion luminescence in the Y/Yb/Er-MOF, thereby providing a sensitive indicator of water vapor concentration changes. The material demonstrates a linear relationship between varying relative humidity (RH) and the corresponding luminescence intensity ratios of I_{500}/I_{660}, with a detection range spanning from 11% to 95%.

In parallel, the macrostructure of the MOF material is a pivotal factor that significantly influences the humidity detection range and determines its sensing capabilities. Two-dimensional (2D) MOF nanosheets, featured by a simpler structure and an abundance of surface active sites relative to their bulk counterparts, have demonstrated the potential to expand the humidity detection range.[63–66] Tan and colleagues successfully produced 2D MOF nanosheets through ultrasonication of synthesized bulk MOFs.[67] These nanosheets were then integrated with seaweed cellulose nanofibrils (CNFs). The resulting composite, TOCNF-MOF, exhibits fluorescence emission characteristic of its aggregation-induced emission (AIE) properties, as depicted in Fig. 2. Capitalizing on the inherent hygroscopic nature of CNFs, the composite's detection range for air humidity extends from 0 to 100% RH. The fluorescence emission intensity of the composite gradually diminishes as the RH increases from 0 to 75%. However, a notable decrease in fluorescence intensity is the pronounced dispersion of the interlayer structure within the aggregated state of MOF nanosheets.

3.2. O_2 sensing

Oxygen detection is of paramount importance in our daily lives, given that oxygen is indispensable for human survival and serves as a vital signifier in a spectrum of sectors, including industrial and medical applications.[68] The need for real-time monitoring of oxygen levels has driven the evolution of sensing materials and methodologies for the precise detection of oxygen. Organic fluorophores, including porphyrin, pyrene, and anthracene, are frequently employed as indicators of oxygen presence. Especially, porphyrins and metalloporphyrins are strongly quenched by oxygen. Porphyrins are a class of macromolecular compounds formed by the joining of four pyrrole rings *via* a hypomethyl bridge (–CH═). Porphyrins can react with oxygen to form peroxides or free radicals, and these products may be further involved in other chemical reactions leading to more complex oxidation processes. Nonetheless, they are often plagued by aggregation-caused quenching (ACQ), which markedly restricts their effectiveness in oxygen sensing applications.

Incorporating oxygen-sensitive groups into the MOF framework, along with utilizing the MOFs' structural attributes to modulate the spacing between fluorescent moieties, has become a principal strategy for curbing ACQ and for enhancing the sensitivity, selectivity, and stability of oxygen sensors. Mesin[69] and colleagues incorporated porphyrin into their optical gas sensor, thereby enabling the detection of oxygen (O_2) and nitrogen oxide (NO). By relying on the oxygen-sensitivity of the $Ru(dpp)_3^{2+}$ complex, the sensor achieved a notably high sensitivity of 10.7. The sensitivity was quantified as the ratio of the fluorescence intensity measured under 100% nitrogen (N_2) *versus* 100% oxygen (O_2) environments. This approach underscores the effectiveness of MOFs in the development of highly responsive and selective oxygen sensing technologies.

Concurrently, Li *et al.*[44] harnessed the MOF structure to mitigate the ACQ effect of the oxygen-sensitive perylene molecules in the context of oxygen detection. By integrating stilbene-containing linkers into the MOF framework, they leveraged the rigid structure of MOF to fine-tune the spacing between perylene molecules, effectively preventing their aggregation. Testing revealed that the developed MOF achieved its peak fluorescence quantum efficiency of 50% when the perylene group concentration was optimized at 1.8%. Importantly, at this concentration, the fluorophore exhibited its maximum sensitivity to oxygen, reaching 58%. Additionally, capitalizing on the high porosity inherent to this MOF structure, the sensor

Published on 26 Qado Dirri 2024. Downloaded by Fail Open on 23/07/2025 10:24:49 AM.

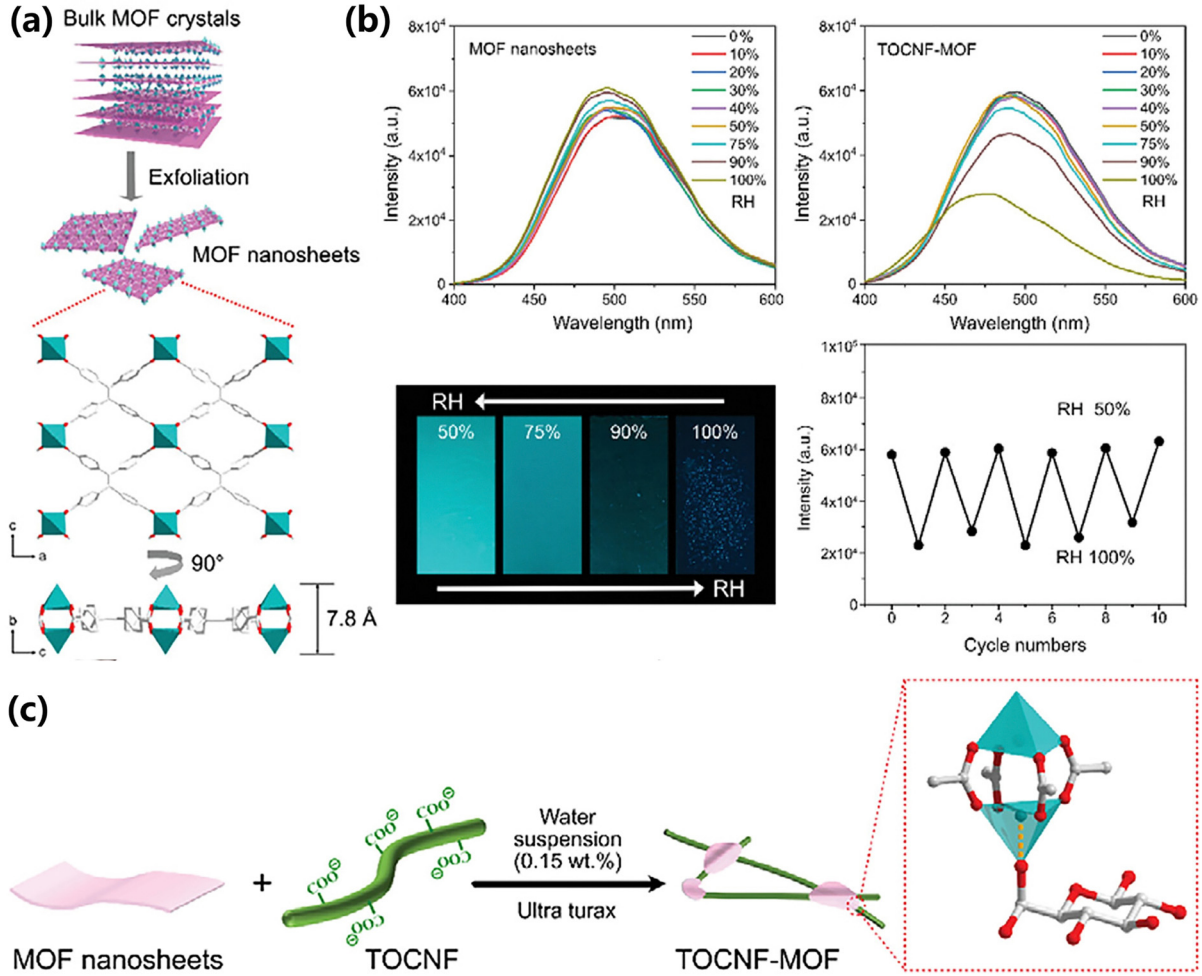

Fig. 2 AIEgen-based fluorescent metal–organic framework nanosheets and seaweed cellulose nanofibrils for humidity sensing.[67] (a) Illustration of the exfoliation of the AIEgen-based bulk MOF crystals into ultrathin 2D nanosheets that consist of monolayer MOF nanosheets with a structure viewed from the [010] and [100] directions. (b) Moisture-sensitive properties of neat MOF nanosheets and the TOCNF-MOF composite film at different humidity levels. (c) Illustration of the process to prepare TOCNF-MOF assembly and the model of the coordination interactions between MOF and TOCNF. Reproduced from ref. 67 with permission from Wiley-VCH GmbH, copyright 2022.

demonstrated an exceptionally fast response, accomplishing the task within seconds—a marked improvement over the 60-second response time reported in Mesin's[69] study.

Building upon the suppression of ACQ, the pursuit of enhanced stability has become the new priority. In a recent breakthrough, Burger *et al.*[70] developed zirconium-based porphyrin metal–organic frameworks (MOFs) that exhibit an extended fluorescence decay time and improved fluorescence quantum yield, oxygen sensitivity, and stability. This enhancement was achieved by meticulously controlling the spacing between porphyrin groups. Within the series of these zirconium-based porphyrin MOFs, the PCN-223 variant has proven to be particularly robust, showing only minor fluctuations in the Stern–Volmer (SV) constants as shown in Fig. 3, which underscores its superior performance in oxygen sensing.

3.3. Sensing of sulfur containing toxic gases

Sulfur is a common element found in fossil fuels, non-ferrous metals, and living organisms. The sources of sulfur are varied and ubiquitous, with activities such as mining, smelting, fuel combustion, chemical synthesis, and even biological metabolism all capable of releasing sulfur-containing toxic gases. These include sulfur oxides, hydrogen sulfide, methyl mercaptan, dimethyl sulfide, and others.[71–73] Among these, sulfur oxides and hydrogen sulfide (H_2S) are the most prevalent.

Sulfur oxides, with SO_2 being a prime example, are the primary contributors to acid rain and are also linked to respiratory diseases in humans. H_2S, known for its rotten egg odor, is a toxic gas that is a strong irritant to the human visual, respiratory, and nervous systems. It also poses a risk of explosion when exposed to open flames or high temperatures. Consequently, detecting sulfur oxides and hydrogen sulfide in the environment is crucial to safeguarding life quality and ensuring safety.

SO_2 emissions can originate from numerous sources, underscoring the strong necessity for continuous, real-time monitoring levels over long periods. Consequently, enhancing the selectivity and sensitivity of SO_2 detection has emerged as a

 This journal is © The Royal Society of Chemistry 2024

Published on 26 Qado Dirri 2024. Downloaded by Fail Open on 23/07/2025 10:24:49 AM.

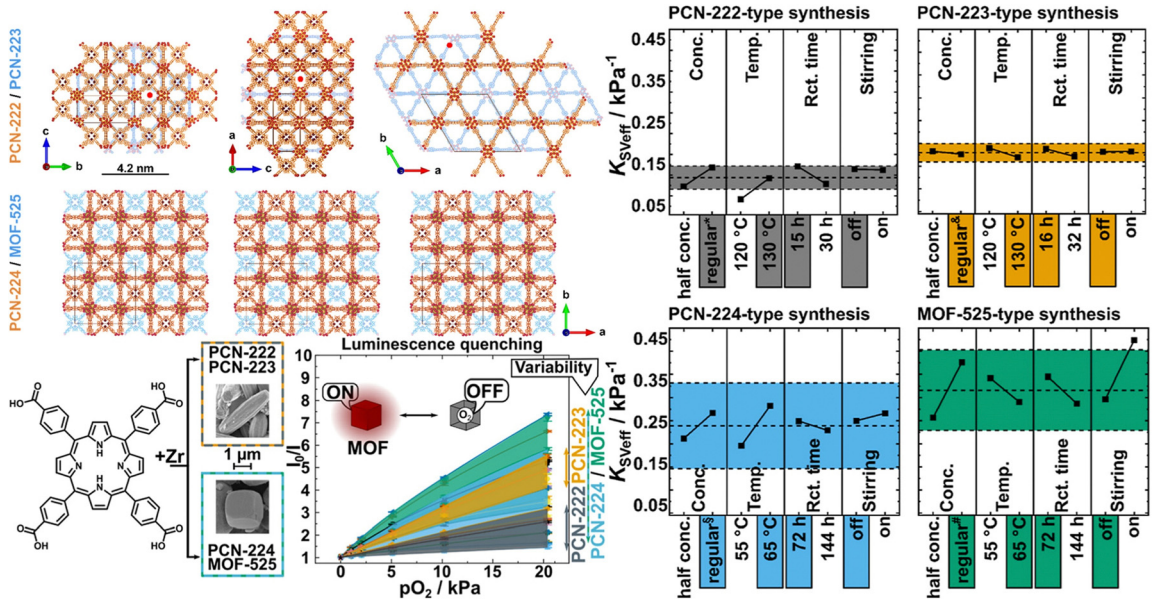

Fig. 3 The structure of zirconium-based porphyrinic metal–organic frameworks and the main effect plots of the DoEs showing the influence of synthesis parameters on the oxygen sensitivity of the materials obtained by the respective synthetic pathway. Reproduced from ref. 70 with permission from American Chemical Society, copyright 2022.

critical challenge in the advancement of SO_2 sensing technology. Lou *et al.*[74] harnessed MOF-5 as a scaffold to incorporate amino functional groups into the MOF, thereby enhancing its interaction with specific gases, as shown in Fig. 4. They integrated MOF-5-NH_2 into a polyvinyl alcohol (PVA) solution, yielding a composite film with exceptional selectivity for SO_2. This composite film, leveraging the chemical reactivity of the $-NH_2$ groups with SO_2, facilitated the qualitative detection of SO_2. However, the data pertaining to its lower limit of detection (LOD) were not thoroughly reported. In another regard, a sensing

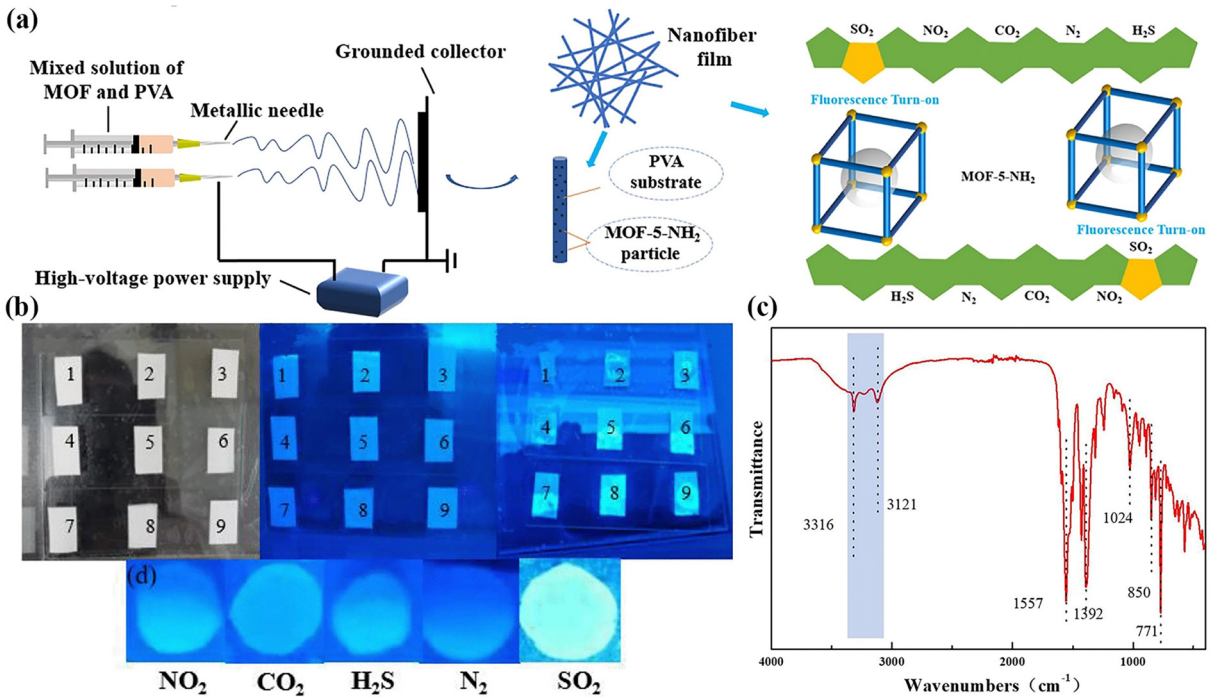

Fig. 4 (a) Schematic diagram of the preparation of MOF-5-NH_2/PVA nanocomposite film; (b) the composite films with MOF-5-NH_2 ratios of 0%, 10%, 15%, 20%, 25%, 30%, 35%, 40% and 45% within and without 365 nm UV lamp irradiation and SO_2 gas environment; (c) the IR spectrum of MOF-5-NH_2. Reproduced from ref. 74 with permission from The Polymer Society, copyright 2022.

Published on 26 Qado Dirri 2024. Downloaded by Fail Open on 23/07/2025 10:24:49 AM.

mechanism that capitalizes on the augmentation of fluorescence intensity offers an alternative and effective method for detecting gases at low concentrations. Valeria *et al.*[75] investigated a distinct Ni(II)-based MOF, utilizing 4,4′-dioxidobiphenyl-3,3′-dicarboxylate (dobpdc) as the organic ligand. Upon interaction with SO_2 and metal centers, the molecular motion of dobpdc is observed to undergo rigidification, leading to an increase in fluorescence intensity. This Ni-MOF demonstrated a robust photoluminescence response under low SO_2 pressure, achieving detection of SO_2 concentrations as low as 4.3 mmol g^{-1} at 298 K and 0.05 bar. By contrast, fluorescence "turn on" mechanism facilitates more accurate detection. Wang *et al.*[76] described a reaction-triggered Ce^{4+}/Tb^{3+} MOF fluorescent probe, utilizing Ce^{4+} as the reactive ion with fluorescence emanating from Tb^{3+}. The energy produced from the reduction reaction between Ce^{4+} and SO_2 or sulfites is harnessed to excite the Tb^{3+} ion, resulting in its fluorescence emission. Sensors for SO_2 based on this principle offer excellent selectivity and sensitivity. The achieved detection limits for this technology were 50 nM for sulfite and 0.093 μM for SO_2, showcasing the effectiveness of this approach in detecting sulfur dioxide at very low concentrations.

In the realm of H_2S detection, achieving high sensitivity and a low LOD are paramount, as even trace amounts of H_2S can be detrimental to human health. Concurrently, enhancing the response speed of toxic gas sensors is crucial for facilitating the swiftest possible emergency response in the event of a leak, thereby mitigating the potential loss of public property. Additionally, practical sensors should aim to reduce fabrication costs; thus, identifying reversible sensing materials presents an effective solution. Currently, the detection of H_2S is addressed through the use of lanthanide-based metal–organic frameworks (Ln-MOFs), copper-based metal–organic frameworks (Cu-MOFs), and MOF composites. Zhu *et al.*[77] have developed a novel sensing platform by growing MOF-5-NH_2 on the surface of Au@Ag nanoparticles (NPs), serving as a dual-probe for both fluorescence and surface-enhanced Raman scattering (SERS). This Au@Ag NPs@MOF-5-NH_2 hybrid system is capable of simultaneously detecting two sulfur-containing gases, H_2S and SO_2, achieving an ultra-low LOD of 2.26 nM by leveraging the SERS[78] and fluorescence "turn-on" mechanisms.

Another report of utilizing fluorescence "turn on" mechanism to achieve high performance H_2S detection was reported by Ghosh *et al.*[79] They introduced a Zr-UiO-66 MOF as a fluorescent probe capable of detecting H_2S in both the gaseous phase and aqueous solutions. The detection mechanism involves a nucleophilic substitution reaction between 4-nitrobenzene functionalized organic ligands and the HS-ion, yielding a hydroxyl-functionalized fluorescent molecule. This fluorescent probe has been effectively employed for the detection of H_2S in both phases. Specifically, H_2S vapor was discerned by monitoring a 2.6-fold increase in fluorescence intensity within a mere six minutes.

It is worth noting that the Cu-MOF is a commonly applied MOF material for the fluorescent detection of H_2S. The combination of copper cation with a luminescent ligand in MOFs to generate a complex will turn off the fluorescence, and after the introduction of H_2S, the copper cation reacts with H_2S to generate CuS, which turns the fluorescence back on. Based on this principle, a variety of Cu-MOFs based H_2S fluorescence gas sensor have been reported with low detection limits and fast detection response. Hou *et al.*[80] proposed to utilize a Cu-MOF based dual mode colorimetric/chemiluminescent (CL) mechanism to achieve sensitive H_2S vapor detection. They synthesized a Cu-MOF with 2,4,6-tris(4-carboxyphenyl)-1,3,5-triazine (TATB) as the ligand *in situ* on a paper substrate, and the porous Cu-TATB, in addition to removing the enhanced adsorption of H_2S, catalyzed the luminescence of luminescent CL system, which was exposed to the volatile sulfur-containing compounds showed a color change (colorimetric) from aqua-blue to green-brown with a detection limit as low as 0.2 μM for the detection of H_2S in breath. In addition, the prepared Cu-TATB@paper could be stored in air for 18 months, showing good stability. In a concurrent development, H_2S vapor detection with regeneration capability and prompt response was achieved using a Cu-MOF based fluorescent MOF material. Marquardt *et al.*[81] reported on a fluorescent MOF material that exhibits a swift response time. They utilized a copper-functionalized MOF-808, which undergoes a color transition from green or blue to brown upon exposure to H_2S gas. This sensing material is entirely regenerable, and its regeneration process is expedited by heating followed by cooling under humid conditions, achieving a response rate within the range of 1.3 to 2.2 minutes. It worth noting that the Cu-based MOF can be regenerated after sensing by applying heat, which significantly enhances the sensor's lifespan and operational longevity.

3.4. Nitride sensing

Gaseous inorganic nitrogen compounds contain various nitrogen oxides and ammonia. Typical gases to be tested are NO_2, NO and NH_3. NO_2 is a reddish-brown toxic gas and a source of the greenhouse effect, while NO is one of the small molecules involved in the functioning of the body's immune system and nervous system, but excessive amounts of NO can cause damage to the body,[82] It is one of the contributing factors to acid rain and haze in the atmosphere.[83] Moreover, NH_3 is a colorless gas with an irritating odor and is highly toxic. Therefore, it is of great importance to detect nitrogen-containing gases effectively with low detection limits and fast response time. The detection of NO and NO_2 typically operates through two primary mechanisms: (1) the alteration of fluorescence emission due to energy or charge transfer between the probe and the analyte; (2) a chemical reaction between the analyte molecule and the probe, leading to the creation or elimination of a fluorophore. Utilizing these mechanisms, fluorescent MOFs have been explored for the development of sensors capable of detecting NO and NO_2 gases.

A typical work utilizing mechanism (1) to achieve effective NO_2 vapor detection is reported by Moscoso *et al.*[22] They synthesized a terbium-based MOF, denoted as Tb(BTC), using benzene-1,3,5-tricarboxylate (BTC) as an organic ligand. NO_2 acts as an electron acceptor, causing the intrinsic fluorescence

 This journal is © The Royal Society of Chemistry 2024

Published on 26 Qado Dirri 2024. Downloaded by Fail Open on 23/07/2025 10:24:49 AM.

of Tb(BTC) to quench by opening a new energy transfer channel from the BTC ligand to the analyte molecule. The sensing sensitivity was further enhanced by the incorporation of the MOF particles into a polymer matrix, which is beneficial for providing adequate accessibility of the analytes into the cages of the sensing material. This approach culminated in the realization of a sub-ppb detection range for nitroaromatic vapors.

Under certain conditions, the concurrent deployment of dual mechanisms can synergistically amplify the sensing performance across multiple dimensions, including sensitivity, selectivity, and response time. Mandal *et al.*[65] enhanced MOF-808 through post-synthetic modification, introducing amine groups *via* ligand grafting. The PET between NO and the MOF is complemented by a swift chemical reaction with the free amino groups present within the MOF, culminating in a rapid fluorescence turn-off response. This MOF, bolstered by the integrated sensing mechanisms, achieved a detection limit of 0.715 μM for NO. The synthesized MOFs are capable of selectively detecting NO in both liquid and gas phases.[84]

Complementing the primary sensing mechanisms, an additional NO gas sensing approach, predicated on fluorophore generation catalyzed by MOFs, has been investigated and deployed. Wang *et al.*[85] have synthesized a copper–cobalt elementally doped metal–organic framework (CuCo-PTC MOF), employing biphenyl-3,4′,5-tricarboxylic acid (H_3PTC) as the organic ligand. This CuCo-PTC MOF catalyzes the oxidation of *o*-phenylenediamine and hydrogen peroxide, yielding a fluorescent fluorophore with yellow emission. In the presence of NO, *o*-phenylenediamine selectively reacts with it, leading to the formation of a non-fluorescent product. By leveraging this reaction-based sensing strategy, Wang *et al.* achieved a detection sensitivity threshold of 0.15 μM for NO and successfully detected endogenous NO within cellular systems.

Beyond nitric NO and nitrogen NO_2, ammonia represents another prevalent toxic nitrogenous compound. The sensing mechanism for ammonia predominantly hinges on its inherent chemical reactivity. Advancing the development of an effective ammonia sensor necessitates achieving a lower detection limit, expedited response time, and enhanced stability. Carboxylic acid, quinoline, and pyridine groups are frequently selected probes known for their propensity to react readily with ammonia (NH_3). Goel *et al.*[86] have integrated inkjet printing technology to fabricate patterned films on flexible substrates such as paper-based polyethylene terephthalate and others, utilizing a suite of transition metal and terbium-based MOF as inks. Notably, two MOF films—Tb-BTC (where BTC denotes benzotricarboxylic acid) and Mn-BDC (with BDC representing benzenedicarboxylic acid)—have demonstrated the capability for fluorescence and colorimetric sensing of ammonia. The ammonia molecules engage in a reaction with the free carboxylic acid groups that are resident within the organic linkers of the MOFs, which results in a fluorescence intensity reduction that correlates linearly with the ammonia concentration. By harnessing the carboxylic acid groups in conjunction with the MOF structure, the sensor has accomplished a LOD of 0.3 ppm for ammonia.

To enhance sensitivity, the 2D MOF structure, recognized for its substantial specific surface area, has been employed for the detection of ammonia gas. Wong *et al.*[87] have incorporated 8-hydroxyquinoline to complex with zinc (forming ZnQ) and subsequently encapsulated and decorated it onto the Zn-BTC MOF. The ensuing 2D nanosheets exhibited fluorescence quenching upon exposure to ammonia gas, achieving a detection limit of 0.27 ppm. The improved sensing performance is largely credited to the surface charge modification of Zn-BTC induced by ZnQ, which confers an increased number of active sites.

Beyond the implementation of innovative MOF structures, the post-synthesis modification of fluorescent MOF materials to enable multiple response mechanisms represents an efficacious strategy for the holistic enhancement of sensing performance. Liu *et al.*[88] have conducted a post-synthesis quaternization of the pyridine group within the Zr(IV) MOF. This modification, attributed to the formation of charge transfer complexes between the pyridine and amine groups, results in a swift color transition from off-white to reddish-brown upon the MOF's exposure to ammonia and various alkylamine vapors. Subsequent to the grafting of diverse polycyclic aromatic hydrocarbons (PAHs) onto the generated N-amino groups, the MOF exhibited intense fluorescence across a spectrum of colors, accompanied by rapid and complete fluorescence quenching in response to ammonia exposure, in addition to the color alteration. The LOD for this sensor was determined to be 7.33 μM.

The detection of NH_3 gas with high sensitivity can also be accomplished through fluorescent MOF-based colorimetric sensors that offer high resolution. Sotirov *et al.*[89] presented a Co(II)-based MOF utilizing homotrimellitic acid as the ligand. Upon integration of this MOF into a poly-D-lactic acid (PDLA) thin film, the resulting sensor exhibited a distinct color transition from pink to purple upon exposure to NH_3. This color change is attributed to the progressive degradation of the MOF structure at elevated pH levels following NH_3 exposure and the concurrent formation of cobalt-ammonia complexes. The original color can be restored by treating the NH_3-exposed sensor with HCl and the sensor demonstrates a LOD of 60 ppm.

Under certain conditions, there is a demand for reversible sensing of NH_3 gas. Consequently, researchers have discovered that the deprotonation property of ammonia, which can be induced by HCl, can be harnessed to achieve reversible ammonia sensing. For example, Chen *et al.*[90] synthesized two lanthanide MOFs, 1-Eu and 1-Tb, utilizing bipyridine tetracarboxylic acid (H4L) as the ligand. The uncoordinated nitrogen atoms on the bipyridine groups and water molecules within the two Ln-MOFs offer Lewis-base sites for detecting heavy metal ions and acid–base vapors. Exposure to HCl vapors results in protonation of the pyridyl nitrogen atoms, leading to fluorescence quenching. Conversely, exposure of the HCl-treated MOFs to NH_3 induces deprotonation, which restores the fluorescence. After undergoing five cycles, no significant reduction in the fluorescence on–off contrast was observed, indicating the sensor's relative stability in the reversible sensing process.

Published on 26 Qado Dirri 2024. Downloaded by Fail Open on 23/07/2025 10:24:49 AM.

3.5. HCl sensing

Hydrogen chloride (HCl) is a colorless and smelly gas at room temperature, posing extreme hazards to both human health and the environment. Additionally, HCl is intensely corrosive in aqueous solution and can form explosive mixtures when combined with air. Consequently, the real-time and precise detection of HCl gas concentrations is of paramount importance for safety and environmental protection.[91]

The detection mechanism for HCl involves the quenching of fluorescence signals due to the protonating ability of HCl molecules.[69,70] This quenching effect is reversible; treating the system with ammonia or organic amine vapors can restore fluorescence. Capitalizing on the protonation capability and leveraging the advantages of MOF materials in the sensing field, fluorescent MOF materials have been developed for HCl detection. These materials offer enhanced sensing performance, including improved sensitivity and a rapid response time. Building upon the aforementioned principles, a multitude of fluorescent MOF-based HCl sensors have been engineered.[88,90] Gao *et al.*[92] synthesized a three-dimensional europium (Eu) MOF, $[Eu_3(OH)(1,3\text{-db})_2(H_2O)_4]$–$3H_2O$ (where 1,3-db represents 1,3-bis(3′,5′-dicarboxyphenyl)benzene), characterized by a Z-shaped $[Eu_3(COO)_8]$ chain and π-electron-rich tricarboxyphenyl tetracarboxylate ligands. In the presence of HCl vapor, the MOF material's red fluorescence emission is completely quenched within 7 minutes. This fluorescence can be subsequently restored by treatment with triethylamine vapor. However, in this study, the concentration of HCl vapor was not quantified.

Toward the goal of more precise and quantitative detection of HCl vapor, Xu *et al.*[93] introduced a porous, three-dimensional, non-interpenetrating fluorescent MOF material, designated as HPU-23, which features a carboxylic acid framework. The material's blue fluorescence signal is quenched upon exposure to HCl vapor due to the protonation effect, culminating in the achievement of a low LOD of 0.389 ppm, as presented in Fig. 5.

Upon encountering molecules that exhibit weak luminescence due to intramolecular nonradiative relaxation, the traditional fluorescence quenching sensing approach became inapplicable. In view of this scenario, the fluorescence "turn-on" mechanism for gas sensing is more applicable leveraged by it showcasing apparent signal variation in the sensing process. For instance, Wang *et al.*[94] constructed two kinds of Co-MOFs, the MOFs were assembled with an amide-functionalized ligand and two heterostructured nitrogen-containing ligands. The fluorescence of the MOF structures was turned on upon encountering with the HCl molecule. This sensing process is reversible, since the emitted fluorescence can be turned off by contacting with triethylamine.

It is worth noting that the strong polarity of HCl also contributes to enhancing the sensitivity of detection. Tang's group[95] discovered that the strongly dipolar HCl, when adsorbed within the MOF channels, stabilizes the excited state of Zn MOF-HCl through dipole–dipole interactions. This stabilization inhibits the pronounced intramolecular charge transfer behavior characteristic of the unique $[M^+\text{–L–}M^-\text{–L–M}]_\infty$ (M = metal cluster, L = ligand) conformation by ligand twisting. As a result, it diminishes the redshift in emission and

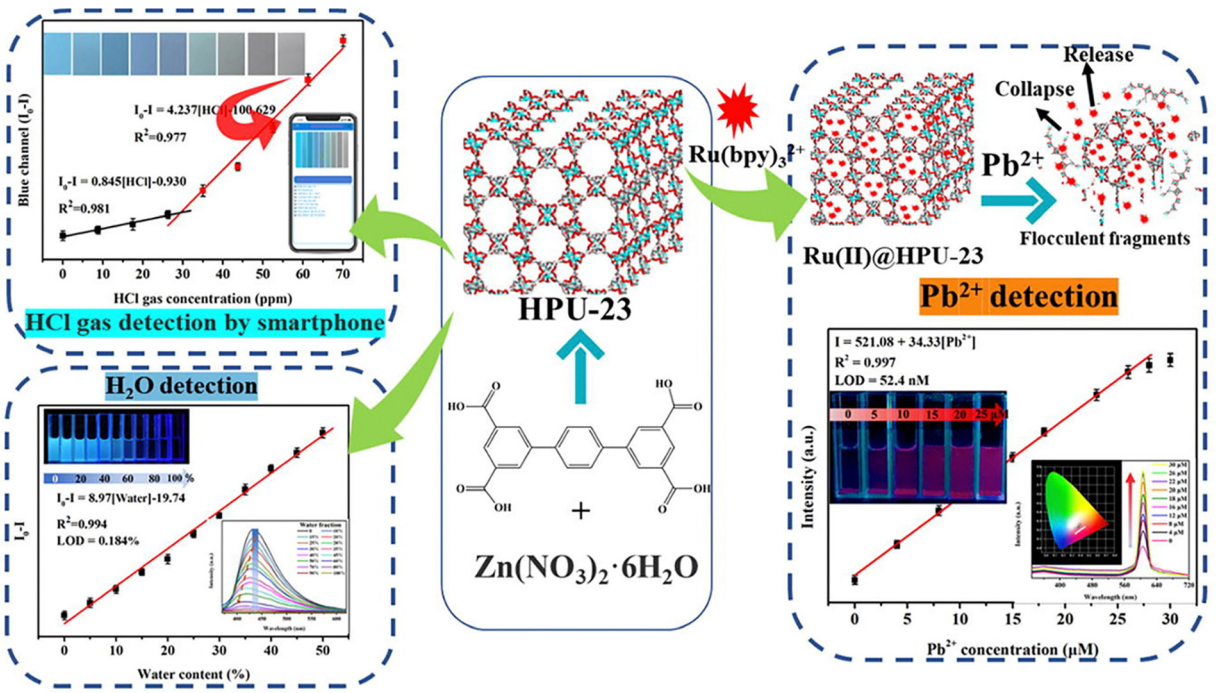

Fig. 5 A novel multifunctional fluorescent sensor HPU-23 is designed for the detection of HCl, trace water and Pb^{2+}. Reproduced from ref. 93 with permission from Elsevier B.V, copyright 2022.

 This journal is © The Royal Society of Chemistry 2024

Published on 26 Qado Dirri 2024. Downloaded by Fail Open on 23/07/2025 10:24:49 AM.

extends the fluorescence lifetime, leading to a calculated LOD of 2.63 ppm.

4. Applications of fluorescent MOF sensors in volatile organic compounds (VOCs)

Volatile organic compounds (VOCs) represent a chemical class whose definition differs across various scientific disciplines. The World Health Organization delineates VOCs as organic compounds exhibiting a boiling point between 50 °C and 250 °C, possessing a saturated vapor pressure above 133.32 kPa at room temperature, and manifesting as vapors in the atmosphere under standard environmental conditions.[96,97] VOCs originate from a multitude of sources, encompassing both natural occurrences and human-induced activities. The majority of these compounds exert negative influences on the environment. Specifically, aromatic and unsaturated hydrocarbons are acknowledged for their considerable impact on ozone formation. Additionally, certain toxic gases, including toluene, have been classified as potent carcinogens, which underscores the imperative to address VOC emissions.[98]

Beyond environmental concerns, VOCs also serve as vital biomarkers for human and plant health. For example, the analysis of VOCs present in exhaled human breath can assist in the early detection of various diseases, including cancer.[99,100] Furthermore, the real-time detection of VOCs can be instrumental in guiding agricultural practices by pinpointing the specific components emitted by plants.[101]

Moreover, the detection of VOCs plays a significant role in safeguarding food safety and public health.[102–104] Therefore, the development of precise, real-time monitoring systems for VOCs is of paramount importance.

In this section, we have showcased the applications of fluorescent MOF-based sensors for the detection of several typical VOCs. Our objectives were to achieve a higher sensitivity, enhanced stability, and improved selectivity.[105]

4.1. Aromatic hydrocarbon sensing

Aromatic hydrocarbons are a class of hydrocarbons that include benzene rings within their molecular structure, with examples such as benzene, toluene, xylene, and styrene. The primary source of these compounds is the waste discharged from industrial processes. Exposure to aromatic hydrocarbons can lead to damage in the human nervous and reproductive systems. The International Agency for Research on Cancer (IARC) has classified benzene, toluene, and xylene as human carcinogens.[106] Consequently, it is imperative to develop effective methods for detecting aromatic hydrocarbons with high sensing performance.

A prevalent approach involves encapsulating a luminescent dye or fluorophore within the porous structure of a MOF, which then elicits a fluorescent response upon interaction with the analyte molecules. The use of fluorescent MOF materials offers distinct advantages in enhancing sensing selectivity. This is attributed to their customizable pore sizes and the ability to design sensitive functional groups, allowing for precise molecular recognition and interaction.

Olorunyomi and colleagues[107] developed a fluorescent MOF material capable of distinguishing methanol from aromatic hydrocarbon vapors through contrasting fluorescence responses. Moreover, within the category of aromatic hydrocarbons, the proposed MOF is able to differentiate toluene from xylene based on selective pore size exclusion. For achieving higher sensitivity, Yang *et al.*[108] proposed another fluorescent MOF, C460@Tb-MOF, for the highly selective sensing of styrene by capitalizing its special sensing process relying on the energy transfer from donor molecule methacrylic acid to the acceptor styrene. In addition to the sensitivity, selectivity is another essential indicator to evaluate an aromatic hydrocarbon gas sensor. Li *et al.*[106] proposed and synthesized a Tb-MOF material that utilizes the trimellitic acid (TMA) ligand as its sensitive site for detecting styrene vapor. The material leverages the unique phenomena of Förster resonance energy transfer (FRET) and Dexter electron transfer, which exclusively occur between styrene and the TMA ligands. This interaction endows the Tb-MOF with the capability to detect styrene with high selectivity. Beyond selectivity, the Tb-MOF also demonstrated outstanding response characteristics. The detection limit for styrene was determined to be as low as 0.0017%, indicating high sensitivity.

4.2. Explosive nitroaromatic compounds detection

Nitro-aromatic compounds (NACs), a class of typical VOC compounds, are primary constituents of powerful explosives. Furthermore, they are recognized as common environmental pollutants. Consequently, the effective detection of NACs holds significant practical importance for environmental conservation and human safety. MOFs are considered a promising probe for NACs due to their ultra-high porosity and tunable structure. Unfortunately, since the saturated vapor pressure of NACs is as low as the ppb level, it is exceedingly difficult to detect NAC gases with such low concentrations of traditional MOF sensors. The inaugural report on NAC gas sensing emerged in 2011, wherein Pramanik *et al.*[109] adeptly utilized a three-dimensional MOF to accomplish solid-state detection of NACs. This was facilitated by a donor–acceptor electron-transfer mechanism involving the aromatic analyte and the microporous MOF, coupled with the MOF's exceptional porosity, which markedly enhanced the sensor's sensitivity. After a significant gap of nearly a decade, a second report on NAC gas detection surfaced. In 2020, Moscoso *et al.*[110] developed a solid-state sensor exhibiting sensitivity to gas-phase NACs. This advancement was achieved by integrating Tb(BTC) within a polymethyl methacrylate (PMMA) substrate material. Capitalizing on the intrinsic merits of the terbium fluorescence moiety, characterized by a high quantum yield and narrow linewidth, along with an ultra-sensitive PET sensing mechanism, the sensor was ultimately capable of detecting NAC vapor under saturated vapor pressure conditions with a sub-ppb detection limit.

4.3. Organic amine sensing

Organic amines are important compounds under the category of VOCs compounds. Aniline, a typical organic amines

Published on 26 Qado Dirri 2024. Downloaded by Fail Open on 23/07/2025 10:24:49 AM.

compound, is extensively utilized in various industrial sectors, including the production of dyes, dye intermediates, rubber, and plastics. However, given its high toxicity as an organic substance, the detection of aniline is crucial for both industrial processes and environmental monitoring. To ensure the safe use of aniline and mitigate potential hazards, aniline detection instruments have become indispensable tools. The accurate detection of trace levels of this toxic gas necessitates sensing materials with enhanced sensitivity, selectivity, and responsiveness.

Regarding the enhancement of selectivity, Yang *et al.*[111] have developed a fluorescent MOF probe known as MECS-2 for highly selectively aniline detection. The high selectivity feature of the sensing process is leveraged by the selective fluorescence enhancement mechanism that relies on host–guest interactions occurring exclusively between aniline and the MOF structure. With the assistance of the open one-dimensional channel of the MOF structure for facilitating the aniline molecule entering, the MECS-2 MOF probe finally achieved a rapid and high selective aniline gas sensing.

In the pursuit of enhanced sensitivity, Che *et al.*[112] prepared the small-size Eu@UiO-66(COOH) obtained by post-synthesis modification (PSM), and generated the film-based fluorescent sensor prepared by crosslinking reaction, as shown in Fig. 6. The small-size MOF structure has features of a large specific surface area and the film is characterized by aniline adsorption. Attributed to these two characters, the Eu@UiO-66(COOH) MOF material showed an ultra-sensitive detection for aniline vapor with 0.086 ppb LOD.

In addition to aniline, biogenic amines (BAs), typically arising from the spoilage processes of organic matter, is another

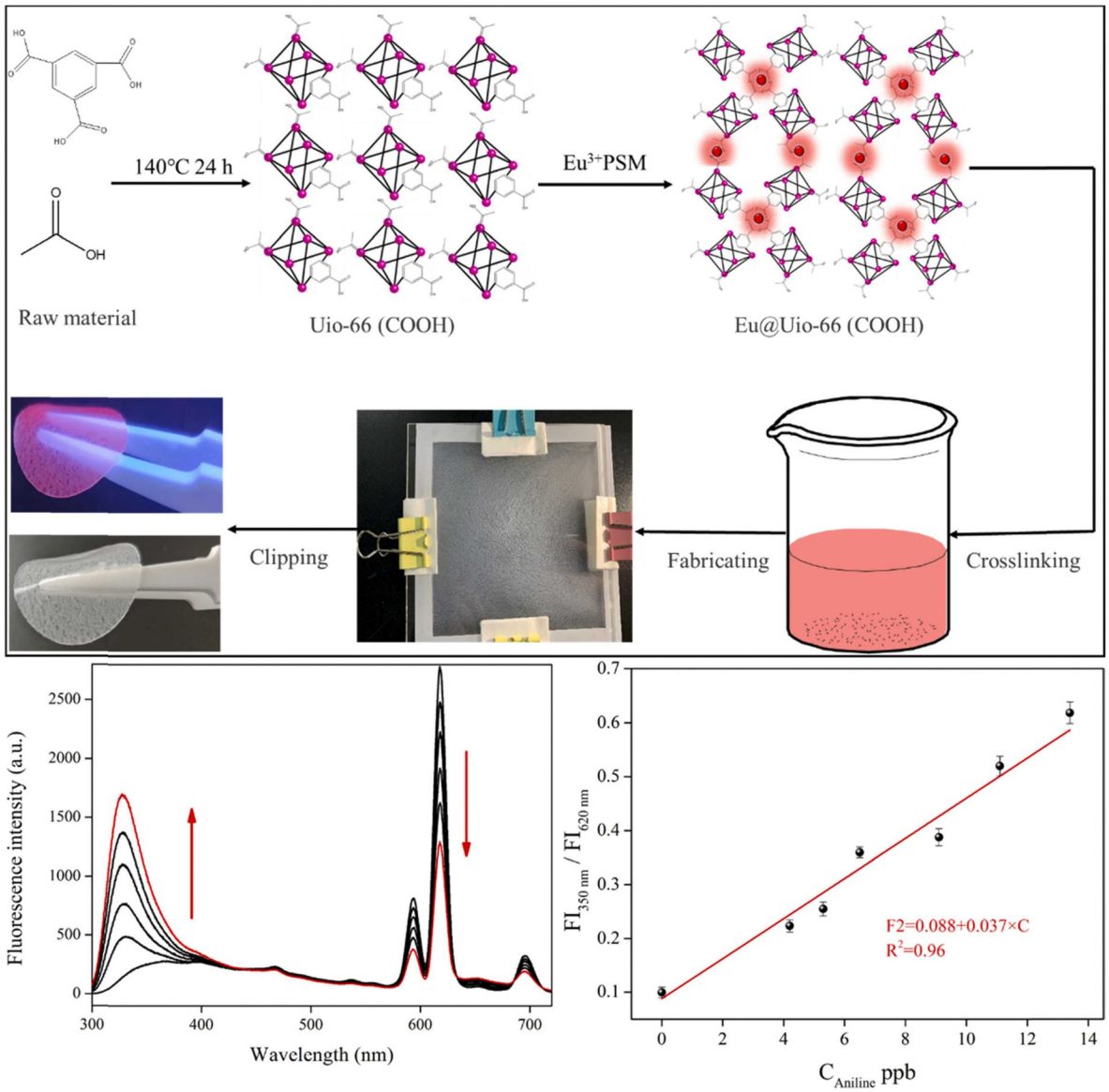

Fig. 6 The schematic diagram of preparation process and the fluorescent sensing in aniline vapor of Eu@UiO-66(COOH) and film sensor. Reproduced from ref. 112 with permission from Elsevier B.V, copyright 2022.

 This journal is © The Royal Society of Chemistry 2024

Published on 26 Qado Dirri 2024. Downloaded by Fail Open on 23/07/2025 10:24:49 AM.

significant category of organic amine compounds. The freshness of food, particularly meat, can be effectively monitored by quantitatively detecting the BAs released during decomposition. Sensors provide real-time and accurate meat freshness monitoring is of great importance to human health. In practical applications, a real-time BA monitoring sensor necessitates a certain level of sensitivity, accuracy, and selectivity to ensure reliable detection. Fluorescent MOF materials have been developed to achieve efficient real-time BA monitoring.

Fluorescence based ratiometric sensing mechanisms, featured by their better accuracy and higher resolution and single wavelength fluorescence sensing, was exploited in MOF based BA detection. For example, Jia *et al.*[113] established a sensory hydrogel and ratiometric fluorescence sensing platform based on Ru@UiO-OH metal–organic skeleton. $Ru(bpy)_3^{2+}$ was encapsulated into UiO-OH to obtain a dual-emission ratiometric fluorescent probe. The developed Ru@UiO-OH presented obvious response to BAs with the phenomenon of enhanced yellow fluorescence, since the MOF would be hydrolyzed and deprotonated under alkaline conditions. In comparison, the red fluorescence of $Ru(bpy)_3^{2+}$ emission was sluggish to BAs, which could act as an internal reference to form a high-resolution color discernment system. Particularly, the ratiometric fluorescence platform based on Ru@UiOOH probes possessed excellent limit of detection toward TMA with 0.389 nM.

Furthermore, an additional sensing mechanism for BAs, characterized by a dual-mode response to fluorescence signals, has been explored. Zhang *et al.*[114] employed a sophisticated multistep tandem functionalization strategy to modify the europium (Eu^{3+})-doped ZnMOF-5-NH_2. This modification involved the incorporation of methacrylic anhydride to introduce unsaturated bonds within the molecular structure. Subsequently, the modified molecule was copolymerized with butyl methacrylate, culminating in the development of europium-based luminescent MOF-derived hybrid polymer films, denoted as Eu-MOF-L@PBMA. Based on its feature of various luminescent responses from the incorporated vapors, a dual-readout orthogonal detection scheme is designed which combines the emission intensity and luminescence lifetime of the Eu-MOF-L@PBMA film. Particularly, it shows the excellent ability to identify ethylenediamine vapors from VOCs and VOAs in terms of its distinct color variation.

4.4. Formaldehyde sensing

Aldehydes and ketones, referring to organic substances that contain a ketone or aldehyde group in the molecule, represent common classes of VOC compounds. Formaldehyde (FA) is the most common volatile aldehyde pollutant. Long-term inhalation of FA can lead to cancer. FA is a ubiquitous emission source, emanating from a spectrum of industries including chemical production, pharmaceuticals, home furnishing, transportation, and beyond. Given its widespread presence, the precise, expeditious, and selective detection of FA is essential for the protection of human health. The exploration of fluorescent MOFs that exhibit heightened sensitivity and selectivity for FA molecules has garnered significant interest. Che *et al.*[115] have synthesized a small-sized Eu-MOF variant, utilizing anhydrous sodium sulfate to modulate particle size, alongside precursors such as $Eu(NO_3)_3{\cdot}6H_2O$ and homobenzoic acid. These particles were integrated into fluorescent films on glass substrates in conjunction with polyvinylidene fluoride (PVDF). Upon exposure to ultraviolet (UV) light, the films exhibited a chromatic shift from red to blue that corresponded with an increase in atmospheric FA concentration. Concurrently, the fluorescence spectrum illustrated a diminution in the emission intensity of Eu^{3+} and an augmentation in the fluorescence intensity of the ligand. This phenomenon is attributed to the electrostatic interactions between FA and Eu-MOF, alongside a disruption in the interaction between the Eu-based MOF and water molecules in the presence of gaseous FA, thereby curtailing energy transfer. As a result, the achieved LOD for FA gas was an impressive 11.8 ppb, indicative of the sensor's extraordinary sensitivity.

Further modifications of the MOF structures have been pursued to attain enhanced responsiveness to the presence of FA molecules. Liu *et al.*[88] have modified the N-amine-treated Zr-bpy metal–organic framework (Zr-bpy-A) with 1-naphthylaldehyde, yielding the post-modified derivative Zr-bpy-ANa. This novel MOF, Zr-bpy-A, exhibits chromic behavior in response to ammonia and amines, attributable to the formation of charge-transfer complexes between electron-deficient pyridinium groups and amino moieties. Additionally, it demonstrates a distinctive chromic response to FA due to Schiff-base condensation with the *N*-amino groups. Capitalizing on these characteristics, the MOF is capable of detecting FA vapors through both colorimetric changes and fluorescence quenching. Consequently, the MOF not only provides a high-contrast fluorescence response to ammonia, amine, and formaldehyde but can also, after adequate training, specifically discern the target gas species.

Beyond structural modifications of MOFs, advanced synthetic techniques are imperative for the efficient fabrication of MOFs with tailored features and functionalities. Bej *et al.*[116] have employed a high-throughput solvothermal process to successfully synthesize two porous MOFs, CMERI-1 and CMERI-2, as presented in Fig. 7. Due to their structural disparities, CMERI-1 exhibits significantly higher sensitivity to FA molecules compared to CMERI-2. Leveraging the light-induced electron transfer (LIET) sensing mechanism and the facile formation of $N{=}CH^-$ groups through the reaction between FA and the $-NH_2$ moieties in CMERI-1, rapid and sensitive FA detection has been realized, with a low LOD of 0.019 ppm.

Furthermore, advanced sensing mechanisms have been continuously developed and demonstrated by researchers to achieve excellent FA sensing performance. For an instance, Li *et al.*[117] designed a novel ZIF-90 MOF (ZIF-90-LW) by combining pre-functionalized 2-allylaminoimidazole ligand and Zn^{2+}. This novel MOF material responded with FA molecule relied on a 2-aza-Cope rearrangement reaction, which possessed high selectivity, high sensitivity and prompt reaction speed simultaneously. This MOF material achieved a superior FA detection with a 2.3 mM LOD and a 28 s response time.

Published on 26 Qado Dirri 2024. Downloaded by Fail Open on 23/07/2025 10:24:49 AM.

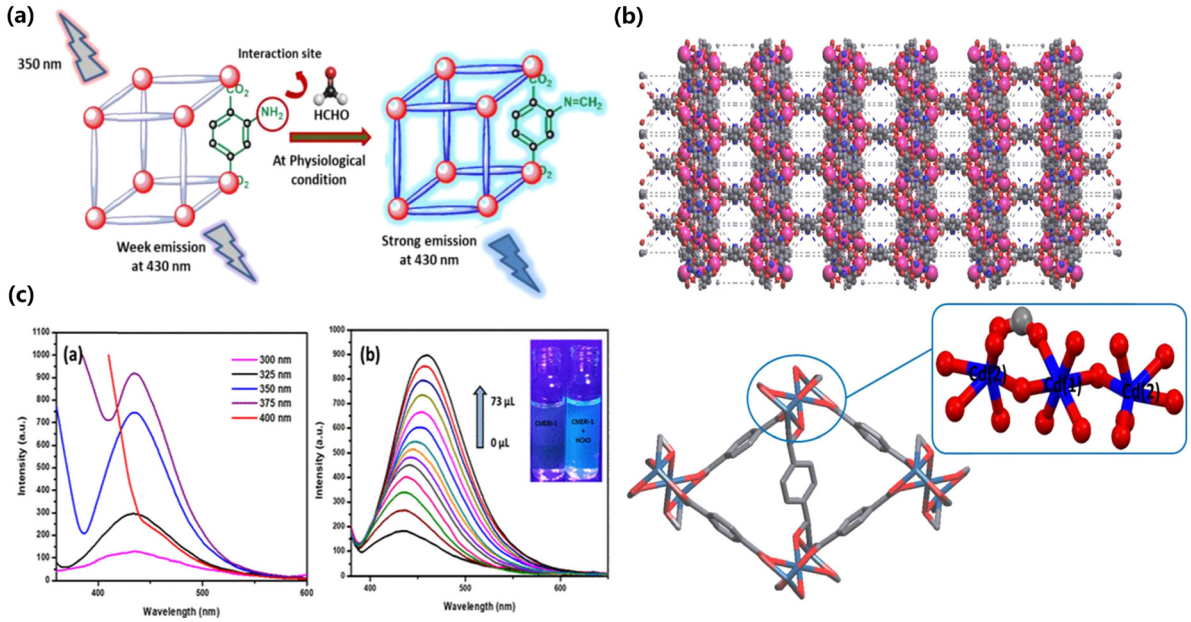

Fig. 7 (a) "Turn-on" Sensing of FA by the d^{10}-MOF (CMERI-1) under physiological conditions, (b) space filling views of the CMERI-1 framework and coordination environment of the Cd(II) atom in the metal–organic framework (CMERI-1), and (c) excitation-dependent fluorescence of CMERI-1 at different wavelengths and fluorescence enhancement after gradual addition of FA. Reproduced from ref. 116 with permission from American Chemical Society, copyright 2021.

4.5. Chemical warfare agent detection

Chemical warfare agents, a subset of volatile organic compounds (VOCs), are specifically engineered to incapacitate or even be lethal to human beings in the context of armed conflict. In laboratory settings, research is typically conducted using analogs that possess structural similarities to actual chemical warfare agents but with attenuated toxicity. 2-Chloroethyl ethyl sulfide (CEES), referred to as half-mustard gas, is an analog of the chemical warfare agent bis(2-chloroethyl)sulfide, commonly known as mustard gas, which is known for its alkylating effects on DNA. Fluorescent probes, attributed to its high sensitivity and rapid response, have been widely applied in the detection of chemical warfare agents.[118,119] Expanding on the foundation laid by fluorescent probes, the advancement of fluorescent MOFs aims to enhance sensing capabilities for the identification of chemical warfare agents. Abuzalat *et al.*[120] encapsulated fluorescein within Zr-BTC to create the composite F@Zr-BTC. Owing to the electron-deficient nature of the guest molecule fluorescein, CEES is capable of transferring electrons to fluorescein, a process that leads to fluorescence quenching and a reduction in fluorescence intensity. This phenomenon enables the detection of trace amounts of CEES, with a LOD achieved by this method being 48 ppb, which is below the lethal dose of CEES (0.2 mg m^{-3}).

5. Conclusions and outlook

In conclusion, the significant research efforts expended over the recent years have highlighted the exceptional performance of fluorescent MOF materials across a spectrum of gas sensing applications. These materials have consistently shown their ability to detect a broad range of gases, from inorganic gases to VOCs. The superior gas sensing performance of the fluorescent MOF material can be attributed to the following distinctive features:

5.1. Inherent porosity

This innate characteristic promotes the diffusion of molecules and boosts interactions with analyte molecules, providing a conducive environment for gas detection.

5.2. Diverse active sites

The presence of open metal sites and the possibility of intermolecular interactions, such as hydrogen bonding and π–π interactions, render the binding of target gas molecules more sensitive and selective.

5.3. Adjustable pore size

The ability to fine-tune the pore dimensions of MOFs is crucial for the efficient separation of molecules, thereby improving the selectivity of the sensing process.

5.4. Host–guest chemistry

Interactions between the host MOFs and guest molecules can lead to measurable changes in various chemical and physical properties, including electrical resistance, mass, magnetism, and color. These changes are instrumental for signal transduction and quantitative analysis.

 This journal is © The Royal Society of Chemistry 2024

Published on 26 Qado Dirri 2024. Downloaded by Fail Open on 23/07/2025 10:24:49 AM.

5.5. Reversible physical adsorption

The process of physical adsorption in MOFs is reversible, taking advantage of their porosity and allowing for the reuse of the fluorescent MOF material.

However, the practical application of fluorescent MOF materials also encounters certain challenges. Although the sensing behaviour of MOF-based materials has been more comprehensively studied, there is still room for improvement. The majority of MOF materials are challenged by inadequate film formation and consistency, which greatly impede their practical utility in gas sensing applications.[121] Furthermore, the strong adsorption characteristic of fluorescent MOFs may, to some extent, impact the gas desorption process, which in turn affects their reusability.[122,123] For the methods of characterization, XRD is a necessary tool to characterize the structural change of the fluorescent MOF material before and after gas sensing, although it is still difficult to conduct it during the sensing process.[43] In addition, most of the reported MOF-based sensors are sensitive to a class of objects, while selective detection of specific species is difficult, especially when the analytes have similar chemical structures. More efforts are needed to design such general strategies for MOF sensors with specific structures. Finally, in-depth studies of structure–luminescence relationships and subject–object interactions are yet to be explored computationally in detail. Compared to research on other MOF applications, such as gas storage, separation, or catalysis, research on MOF-based luminescent probes or chemosensors is still in its infancy. Nanoscale luminescent MOFs have good sensing potential in living cells, while the idea of mounting MOFs into devices, such as fabricating MOF films or membranes, is still in its early stages. Although luminescent MOF-based sensors have shown excellent performance under laboratory conditions, a great deal of research and development is still needed to commercialise the technology.

As the demand for efficient and precise gas detection escalates, the importance of fluorescent MOF materials in gas sensors is set to increase significantly. With keen interest, we anticipate the forthcoming advancements in this field, which are expected to further expedite the practical deployment of fluorescent MOF materials in the realm of gas sensing.

Data availability

No primary research results, software or code have been included and no new data were generated or analysed as part of this review.

Conflicts of interest

There are no conflicts to declare.

Acknowledgements

This work was supported by the National Key Research and Development Program of China (2022YFB3203500) and the National Natural Science Foundation of China [Grant No. 62022085 and 62301544].

Notes and references

1 G. Neri, *Chemosensors*, 2015, **3**, 1–20.
2 Y. Tang, J. Chen, H. Wu, J. Yu, J. Jia, W. Xu, Y. Fu, Q. He, H. Cao and J. Cheng, *Dyes Pigm.*, 2020, **172**, 107798.
3 J. N. O. Amu-Darko, S. Hussain, M. Y. Wang, S. Y. Lei, A. A. Alothman, S. Mohammad, G. J. Qiao and G. W. Liu, *Sens. Actuators, B*, 2024, **407**, 135464.
4 Y. X. Zhai, J. Y. Ye, Y. B. Zhang, K. Z. Zhang, E. Zhan, X. D. Zhang and Y. Q. Yang, *Chem. Eng. J.*, 2024, **484**, 149286.
5 L. Dong, C. Deng, C. He, L. Shi, Y. Fu, D. Zhu, H. Cao, Q. He and J. Cheng, *Sens. Actuators, B*, 2013, **180**, 28–34.
6 L. Wang and J. Song, *Sens. Actuators, A*, 2023, **362**, 114676.
7 Y. Fu, L. Shi, D. Zhu, C. He, D. Wen, Q. He, H. Cao and J. Cheng, *Sens. Actuators, B*, 2013, **180**, 2–7.
8 Y. Yu, W. Xu, Y. Fu, H. Cao, Q. He and J. Cheng, *Dyes Pigm.*, 2020, **172**, 107852.
9 D. Zhu, Q. He, H. Cao, J. Cheng, S. Feng, Y. Xu and T. Lin, *Appl. Phys. Lett.*, 2008, **93**, 261909.
10 W. Song, X. Zhai, J. Shi, X. Zou, Y. Xue, Y. Sun, W. Sun, J. Zhang, X. Huang, Z. Li, T. Shen, Y. Li, C. Zhou, M. Holmes, Y. Gong and M. Povey, *Food Chem.*, 2024, **434**, 137423.
11 M. D. Allendorf, C. A. Bauer, R. K. Bhakta and R. J. T. Houk, *Chem. Soc. Rev.*, 2009, **38**, 1330–1352.
12 M. Kamalzare, *Physicochemical Aspects of Metal-Organic Frameworks: A New Class of Coordinative Materials*, Springer International Publishing, Cham, 2023, pp. 15–30.
13 C. H. Shim, S. Oh, S. Lee, G. Lee and M. Oh, *RSC Adv.*, 2023, **13**, 8220–8226.
14 H. Xu, K. Ye, K. Zhu, J. Yin, J. Yan, G. Wang and D. Cao, *Dalton Trans.*, 2020, **49**, 5646–5652.
15 M. Li, W. Li, S. Zhang, Y. Li, F. Liu, C. Zhao and Y. Wang, *Chem. Ind. Eng. Prog.*, 2021, **40**, 415–426.
16 L. Wang, J. Huang, Z. Li, Z. Han and J. Fan, *Polymers*, 2023, **15**, 1950.
17 C. Wu, K. Zhang, H. Wang, Y. Fan, S. Zhang, S. He, F. Wang, Y. Tao, X. Zhao, Y.-B. Zhang, Y. Ma, Y. Lee and T. Li, *J. Am. Chem. Soc.*, 2020, **142**, 18503–18512.
18 G.-E. Wang and G. Xu, *Sci. Bull.*, 2022, **67**, 2381–2383.
19 Y. Zeng, C. Zhang, D. Du, Y. Li, L. Sun, Y. Han, X. He, J. Dai and L. Shi, *Acta Biomater.*, 2022, **145**, 43–51.
20 C. Arul, K. Moulaee, N. Donato, D. Iannazzo, N. Lavanya, G. Neri and C. Sekar, *Sens. Actuators, B*, 2021, **329**, 129053.
21 E. H. Kwon, M. Kim, C. Y. Lee, M. Kim and Y. D. Park, *ACS Appl. Mater. Interfaces*, 2022, **14**, 10637–10647.
22 F. G. Moscoso, J. Almeida, A. Sousaraei, T. Lopes-Costa, A. M. G. Silva, J. Cabanillas-Gonzalez, L. C. Silva and J. M. Pedrosa, *Mol. Syst. Des. Eng.*, 2020, **5**, 1048–1056.
23 K. Roztocki, V. Bon, I. Senkovska, D. Matoga and S. Kaskel, *Chem. – Eur. J.*, 2022, **28**, e202202255.

Published on 26 Qado Dirri 2024. Downloaded by Fail Open on 23/07/2025 10:24:49 AM.

24 H. Yuan, N. Li, W. Fan, H. Cai and D. Zhao, *Adv. Sci.*, 2022, **9**, 2104374.
25 X. Zhao and X. Miao, *Coord. Chem. Rev.*, 2024, **502**, 215611.
26 Y.-P. Li, S.-N. Li, Y.-C. Jiang, M.-C. Hu and Q.-G. Zhai, *Chem. Commun.*, 2018, **54**, 9789–9792.
27 Z. Shen, W. Li, W. Tang, X. Jiang, K. Qi, H. Liu, W. Xu, W. Xu, S. Zang, K. Zhen, H. Li, Q. He, M. Tu, J. Cheng, Z. Fan and Y. Fu, *Adv. Funct. Mater.*, 2024, 2401631.
28 N. Ding, T. Liu, H. Peng, J. Liu, L. Ding and Y. Fang, *Sci. Bull.*, 2023, **68**, 546–548.
29 M. Zhang, G. Feng, Z. Song, Y.-P. Zhou, H.-Y. Chao, D. Yuan, T. T. Y. Tan, Z. Guo, Z. Hu, B. Z. Tang, B. Liu and D. Zhao, *J. Am. Chem. Soc.*, 2014, **136**, 7241–7244.
30 H.-Y. Li, S.-N. Zhao, S.-Q. Zang and J. Li, *Chem. Soc. Rev.*, 2020, **49**, 6364–6401.
31 M. Gutierrez, Y. Zhang and J. C. Tan, *Chem. Rev.*, 2022, **122**, 10438–10483.
32 X. Xiao, Y. Chen, J.-R. Tao, C. Gao, X.-M. Li, J. Sun and C. M. Jin, *J. Mol. Struct.*, 2024, **1300**, 137311.
33 L. Fan, J. Zhang, Y. Zhao, C. Sun, W. Li and Z. Chang, *Microchem. J.*, 2024, **196**, 109712.
34 X.-C. Yang, S.-Q. Fu, Q.-L. Li, Z. Jiao, J.-T. Zhao, Y. Guo, Z.-J. Zhang, S. Gao and L.-L. Cheng, *Chem. Eng. J.*, 2023, **465**, 142869.
35 Y. Lei, Y. Gao, Y. Xiao, P. Huang and F.-Y. Wu, *Sens. Actuators, B*, 2023, **396**, 134553.
36 Y. Zhang, S. Yuan, G. Day, X. Wang, X. Yang and H.-C. Zhou, *Coord. Chem. Rev.*, 2018, **354**, 28–45.
37 S. Jindal, G. Anjum, V. K. Maka and J. N. Moorthy, *Nanoscale*, 2021, **13**, 9668–9677.
38 X. L. Guo, N. S. Zhu, S. P. Wang, G. H. Li, F. Q. Bai, Y. Li, Y. H. Han, B. Zou, X. B. Chen, Z. Shi and S. H. Feng, *Angew. Chem., Int. Ed.*, 2020, **59**, 19716–19721.
39 F. Sanchez, M. Gutierrez and A. Douhal, *ACS Appl. Mater. Interfaces*, 2023, **15**, 56587–56599.
40 Y. Zhao, H. Hao, H. Wang, L. Sun, N. Zhang, X. Zhang and J. Liang, *Microchem. J.*, 2023, **190**, 108626.
41 S. Geranmayeh, M. Mohammadnejad and A. Abbasi, *J. Fluoresc.*, 2023, **33**, 1017–1026.
42 Q. Yu, Z. Li, Q. Cao, S. Qu and Q. Jia, *TrAC, Trends Anal. Chem.*, 2020, **129**, 115939.
43 Z. Shen, W. Li, W. Tang, X. Jiang, K. Qi, H. Liu, W. Xu, W. Xu, S. Zang, K. Zhen, H. Li, Q. He, M. Tu, J. Cheng, Z. Fan and Y. Fu, *Adv. Funct. Mater.*, 2024, 2401631.
44 J. Li, S. Yuan, J.-S. Qin, L. Huang, R. Bose, J. Pang, P. Zhang, Z. Xiao, K. Tan, A. V. Malko, T. Cagin and H.-C. Zhou, *ACS Appl. Mater. Interfaces*, 2020, **12**, 26727–26732.
45 Z. Zhang, J. Zhou, X. Chen, F. Fang, S. Y. Wang, S. S. Zhang, L. Du and Q. H. Zhao, *Inorg. Chem.*, 2023, **62**, 5972–5983.
46 J. Xiong, Y. F. Xiao, J. M. Liang, J. Sun, L. X. Gao, Q. J. Zhou, D. Hong and K. J. Tan, *Spectrochim. Acta, Part A*, 2023, **285**, 121863.
47 Y. Fu, J. Yao, W. Xu, T. Fan, Q. He, D. Zhu, H. Cao and J. Cheng, *Polym. Chem.*, 2015, **6**, 2179–2182.
48 L. Chen, Y. Gao, Y. Fu, D. Zhu, Q. He, H. Cao and J. Cheng, *RSC Adv.*, 2015, **5**, 29624–29630.
49 H. Y. Niu, J. W. Liu, H. M. O'Connor, T. Gunnlaugsson, T. D. James and H. Zhang, *Chem. Soc. Rev.*, 2023, **52**, 2322–2357.
50 Q. Chen, J. X. Liu, S. J. Liu, J. Zhang, L. F. He, R. Y. Liu, H. Jiang, X. Y. Han and K. Zhang, *Anal. Chem.*, 2023, 4390–4394.
51 F. Yang, D. Lin, L. Pan, J. W. Zhu, J. J. Shen, L. Yang and C. L. Jiang, *Anal. Chem.*, 2021, **93**, 14506–14513.
52 X. R. Shi, C. X. Yin, Y. B. Zhang, Y. Wen and F. J. Huo, *Sens. Actuators, B*, 2019, **285**, 368–374.
53 N. C. Burtch, H. Jasuja and K. S. Walton, *Chem. Rev.*, 2014, **114**, 10575–10612.
54 S. Ding, J. Wan, Y. Ma, Y. Wang, M. Pu, X. Li and J. Sun, *J. Hazard. Mater.*, 2021, **411**, 125194.
55 K. Yu, G. Y. Zhang, H. N. Chai, L. J. Qu, D. Shan and X. J. Zhang, *Sens. Actuators, B*, 2022, **362**, 131808.
56 K. Wu, T. Fei and T. Zhang, *Nanomaterials*, 2022, **12**, 4208.
57 A. Garg, M. Almasi, R. Saini, D. R. Paul, A. Sharma, A. Jain and I. P. Jain, *Environ. Sci. Pollut. Res.*, 2023, **30**, 98548–98562.
58 L. Chen, J.-W. Ye, H.-P. Wang, M. Pan, S.-Y. Yin, Z.-W. Wei, L.-Y. Zhang, K. Wu, Y.-N. Fan and C.-Y. Su, *Nat. Commun.*, 2017, **8**, 15985.
59 P. Anilkumar, L. Cao, J.-J. Yu, K. N. Tackett II, P. Wang, M. J. Meziani and Y.-P. Sun, *Small*, 2013, **9**, 545–551.
60 B. Li, T. Suo, S. Xie, A. Xia, Y.-J. Ma, H. Huang, X. Zhang and Q. Hu, *TrAC, Trends Anal. Chem.*, 2021, **135**, 116163.
61 J.-X. Wu and B. Yan, *Dalton Trans.*, 2017, **46**, 7098–7105.
62 Z. Wang, G. Sun, J. Chen, Y. Xie, H. Jiang and L. Sun, *Chemosensors*, 2022, **10**, 66.
63 Q. Li, Q. Wang, Y. Li, X. Zhang and Y. Huang, *Anal. Methods*, 2021, **13**, 2066–2074.
64 Q. Liu, X. Li, Y. Wen, Q. Xu, X.-T. Wu and Q.-L. Zhu, *Adv. Mater. Interfaces*, 2020, **7**, 2000813.
65 Y. Liu, M. Liu, S. Shang, W. Gao, X. Wang, J. Hong, C. Hua, Z. You, Y. Liu and J. Chen, *ACS Appl. Mater. Interfaces*, 2023, **15**, 16991–16998.
66 Y. Xie, X. Wu, Y. Shi, Y. Peng, H. Zhou, X. Wu, J. Ma, J. Jin, Y. Pi and H. Pang, *Small*, 2024, **20**, 2305548.
67 F. Tan, L. Zha and Q. Zhou, *Adv. Mater.*, 2022, **34**, 2201470.
68 L. Zhang, F. Lin, M. Ye, D. Tian, J. Jin, Y. Huang, Y. Jiang, Y. Wang and X. Chen, *Sens. Actuators, B*, 2021, **346**, 130566.
69 R. Mesin and C.-S. Chu, *Chemosensors*, 2023, **11**, 454.
70 T. Burger, M. V. Hernandez, C. Carbonell, J. Rattenberger, H. Wiltsche, P. Falcaro, C. Slugovc and S. M. Borisov, *ACS Appl. Nano Mater.*, 2023, **6**, 248–260.
71 L. A. Kalinina, G. I. Shirokova, Y. N. Ushakova, E. G. Fominykh, O. V. Medvedeva and I. V. Murin, *Glass Phys. Chem.*, 2005, **31**, 346–351.
72 N. Ploysongsri and V. Ruangpornvisuti, *J. Sulfur Chem.*, 2021, **42**, 383–396.
73 H. Vovusha, R. G. Amorim, H. Bae, S. Lee, T. Hussain and H. Lee, *Mater. Today Chem.*, 2023, **30**, 101543.
74 C.-W. Lou, X. Zhang, Y. Wang, X. Zhang, B.-C. Shiu, T.-T. Li and J.-H. Lin, *J. Polym. Res.*, 2022, **29**, 114.
75 V. B. López-Cervantes, D. W. Kim, J. L. Obeso, E. Martínez-Ahumada, Y. A. Amador-Sánchez, E. Sánchez-González,

 This journal is © The Royal Society of Chemistry 2024

Published on 26 Qado Dirri 2024. Downloaded by Fail Open on 23/07/2025 10:24:49 AM.

C. Leyva, C. S. Hong, I. A. Ibarra and D. Solis-Ibarra, *Nanoscale*, 2023, **15**, 12471–12475.
76 L. Wang and Y. Chen, *Chem. Commun.*, 2020, **56**, 6965–6968.
77 A. Zhu, S. Ali, T. Jiao, Z. Wang, Y. Xu, Q. Ouyang and Q. Chen, *Food Chem.*, 2023, **420**, 136095.
78 J. Hu, G. J. Chen, C. Xue, P. Liang, Y. Xiang, C. Zhang, X. Chi, G. Liu, Y. Ye, D. Cui, D. Zhang, X. yu, H. Dang, W. Zhang, J. Chen, Q. Tang, P. Guo, H.-P. Ho, Y. Li, L. Cong and P. P. Shum, *Light: Sci. Appl.*, 2024, **13**, 52.
79 S. Ghosh and S. Biswas, *Dalton Trans.*, 2021, **50**, 11631–11639.
80 Y. Hou, C. C. Lv, W. Liu, Y. L. Guo, Y. Jin, B. X. Li, Y. Zhang and Y. C. Liu, *Sens. Actuators, B*, 2022, **352**, 131008.
81 N. Marquardt, M. Dahlke and A. Schaate, *ChemPlusChem*, 2023, **88**, e202300109.
82 B. Almeida, K. E. Rogers, O. K. Nag and J. B. Delehanty, *ACS Sens.*, 2021, **6**, 1695–1703.
83 J. Lin, W. Ho, X. Qin, C.-F. Leung, V. K.-M. Au and S.-C. Lee, *Small*, 2022, **18**, 2105484.
84 W. Mandal, D. Majumder, S. Fajal, S. Let, M. M. M. Shirolkar and S. K. K. Ghosh, *Mol. Syst. Des. Eng.*, 2023, **8**, 756–766.
85 M. Wang, H. Dong, Y. Zhang, X. Zhu, M. Gu, Q. Zhu, X. Miao, Y. Zhou and M. Xu, *Microchim. Acta*, 2022, **189**, 263.
86 P. Goel, S. Singh, H. Kaur, S. Mishra and A. Deep, *Sens. Actuators, B*, 2021, **329**, 129157.
87 D. Wong, A. Phani, S. Homayoonnia, S. S. Park, S. Kim and O. Abuzalat, *Adv. Mater. Interfaces*, 2022, **9**, 2102086.
88 X.-Y. Liu, X.-M. Yin, S.-L. Yang, L. Zhang, R. Bu and E.-Q. Gao, *ACS Appl. Mater. Interfaces*, 2021, **13**, 20380–20387.
89 S. Sotirov, S. Demirci, M. Marudova and N. Sahiner, *IEEE Sens. J.*, 2022, **22**, 3903–3910.
90 L. Chen, C.-L. Wang, C.-Y. Zhu, P. Li, W. Gao, J.-Y. Li and X.-M. Zhang, *J. Solid State Chem.*, 2022, **314**, 123423.
91 Y. Ma, Y. He, X. Yu, C. Chen, R. Sun and F. K. Tittel, *Sens. Actuators, B*, 2016, **233**, 388–393.
92 J.-P. Gao, R.-X. Yao, X.-H. Chen, H.-H. Li, C. Zhang, F.-Q. Zhang and X.-M. Zhang, *Dalton Trans.*, 2021, **50**, 1690–1696.
93 X. Xu, H. Li and Z. Xu, *Chem. Eng. J.*, 2022, **436**, 135028.
94 L. Wang, J. Cheng, N. Liu, H. Zou, H. Yan, J. Lu, H. Liu, Y. Li, J. Dou and S. Wang, *Inorg. Chem.*, 2023, **62**, 2083–2094.
95 Z.-H. Zhu, Z. Ni, H.-H. Zou, G. Feng and B. Z. Tang, *Adv. Funct. Mater.*, 2021, **31**, 2106925.
96 R. Epping and M. Koch, *Molecules*, 2023, **28**, 1598.
97 L. Mølhave and G. D. Nielsen, *Indoor Air*, 1992, **2**, 65–77.
98 S. Pan, Y. Choi, A. Roy, X. Li, W. Jeon and A. H. Souri, *Atmos. Environ.*, 2015, **120**, 404–416.
99 L. P. Huang, Y. J. Zhu, C. S. Xu, Y. Cai, Y. D. Yi, K. Li, X. Q. Ren, D. F. Jiang, Y. C. Ge, X. H. Liu, W. J. Sun, Q. W. Zhang and Y. Wang, *ACS Sens.*, 2022, **7**, 1439–1450.
100 Z. J. Zhang, P. W. Li, L. P. Liu, L. H. Ru, H. X. Tang and W. S. Feng, *J. Solid State Chem.*, 2022, **305**, 122623.
101 H. Chen, Z. You, X. Wang, Q. Qiu, Y. Ying and Y. Wang, *Chem. Eng. J.*, 2022, **446**, 137098.
102 M.-M. Pan, D. Feng, Y. Ouyang, D. Yang, X. Yu, L. Xu and I. Willner, *Sens. Actuators, B*, 2022, **358**, 131482.
103 S. Zhang, L. Li, Y. Lu, J. Zhang, D. Liu, D. Hao, X. Zhang, L. Tian, L. Xiong and J. Huang, *J. Mater. Chem. C*, 2022, **10**, 5497–5504.
104 Z. Hu, S. Pramanik, K. Tan, C. Zheng, W. Liu, X. Zhang, Y. J. Chabal and J. Li, *Cryst. Growth Des.*, 2013, **13**, 4204–4207.
105 Y. Shen, A. Tissot and C. Serre, *Chem. Sci.*, 2022, **13**, 13978–14007.
106 L. Feng, C. Dong, M. Li, L. Li, X. Jiang, R. Gao, R. Wang, L. Zhang, Z. Ning, D. Gao and J. Bi, *J. Hazard. Mater.*, 2020, **388**, 121816.
107 J. F. Olorunyomi, M. M. Sadiq, M. Batten, K. Konstas, D. Chen, C. M. Doherty and R. A. Caruso, *Adv. Opt. Mater.*, 2020, **8**, 2000961.
108 J. Yang, C. Ren, M. Liu, W. Li, D. Gao, H. Li and Z. Ning, *Molecules*, 2023, **28**, 4919.
109 S. Pramanik, C. Zheng, X. Zhang, T. J. Emge and J. Li, *J. Am. Chem. Soc.*, 2011, **133**, 4153–4155.
110 F. G. Moscoso, J. Almeida, A. Sousaraei, T. Lopes-Costa, A. M. G. Silva, J. Cabanillas-Gonzalez, L. Cunha-Silva and J. M. Pedrosa, *J. Mater. Chem. C*, 2020, **8**, 3626–3630.
111 F.-P. Yang, Q.-T. He, H. Jiang, Z. Li, W. Chen, R.-L. Chen, X.-Y. Tang, Y.-P. Cai and X.-J. Hong, *Inorg. Chem.*, 2022, **61**, 10844–10851.
112 H. C. Che, S. L. Yan, Y. L. Nie, X. K. Tian and Y. Li, *J. Hazard. Mater.*, 2022, **435**, 129016.
113 P. Jia, X. He, J. Yang, X. Sun, T. Bu, Y. Zhuang and L. Wang, *Sens. Actuators, B*, 2023, **374**, 132803.
114 Z. Zhang, W. Ma and B. Yan, *Colloids Surf., A*, 2022, **648**, 129416.
115 H. Che, Y. Li, X. Tian, C. Yang, L. Lu and Y. Nie, *J. Hazard. Mater.*, 2021, **410**, 124624.
116 S. Bej, S. Mandal, A. Mondal, T. K. Pal and P. Banerjee, *ACS Appl. Mater. Interfaces*, 2021, **13**, 25153–25163.
117 M. Li, A. Shen, Y. Liang, H. Zhen, X. Hao, X. Liu, X. Sun and Y. Yang, *Anal. Methods*, 2020, **12**, 3748–3755.
118 H. Jiang, P. Wu, Y. Zhang, Z. Jiao, W. Xu, X. Zhang, Y. Fu, Q. He, H. Cao and J. Cheng, *Anal. Methods*, 2017, **9**, 1748–1754.
119 Y. Fu, J. Chen, H. Sun, K. Li, W. Xu, Q. He, A. Facchetti and J. Cheng, *Sens. Actuators, B*, 2021, **331**, 129397.
120 O. Abuzalat, S. Homayoonnia, D. Wong, H. R. Tantawy and S. Kim, *Dalton Trans.*, 2021, **50**, 3261–3268.
121 J. Zheng, L. Chen, Y. Kuang and G. Ouyang, *Small*, 2024, 2307976.
122 A. Yu and X. Wang, *J. Mol. Struct.*, 2024, **1295**, 136624.
123 X. Yan, J. Chen, X. Su, J. Zhang, C. Wang, H. Zhang, Y. Liu, L. Wang, G. Xu and L. Chen, *Angew. Chem.*, 2024, e202408189, DOI: **10.1002/anie.202408189**.